PHYSICAL REVIEW B VOLUME 39, NUMBER 8 15 MARCH 1989-I

Shallow positron traps in GaAs

K. Saarinen, P. Hautojärvi, and A. Vehanen
Laboratory of Physics, Helsinki University of Technology, SF-02150 Espoo 15, Finland

R. Krause and G. Dlubek
Sektion Physik, Martin-Luther-Universität Halle, DDR-4020 Halle, German Democratic Republic
(Received 26 August 1988)

Positron annihilation in GaAs at low temperatures has been studied with positron-lifetime and diffusion-length measurements. The lifetime results show that in addition to vacancy-type deep traps, positron trapping with a lifetime very close to the bulk value of 230 ps occurs below 200 K. This is observed together with a strong decrease in the positron-diffusion length from 1500 to 800 Å measured with a slow-positron beam. The results give direct evidence on positron localization at shallow traps in GaAs. A Rydberg state around a negative point charge is suggested for the origin of the shallow trap. The detrapping analysis of both lifetime and diffusion-length data yields a binding energy of 43±5 meV for the positron bound to these negative centers. This value is in good agreement with the binding energies of electrons and holes to the shallow levels in GaAs.

I. INTRODUCTION

Positrons in solids are strongly repelled by positive ion cores. Open-volume defects act as attractive centers, where positrons can get trapped with subsequent changes in their annihilation characteristics. Due to the reduced electron density in these defects, the lifetime of trapped positrons increases and the electron-positron momentum distribution narrows.[1,2]

Positron traps are shallow, if the binding energy is small ($\ll 1$ eV), and consequently the positron wave function is only weakly localized. The annihilation characteristics of the positrons in shallow traps are practically the same as for free positrons in the bulk. Because of small binding energies, shallow traps are effective only at low temperatures, while at higher temperatures positrons are detrapped. In metals, shallow traps have often been called forth to explain the results, when positron trapping and annihilation have shown unexpected temperature behavior.[3-7] Dislocation lines,[4,6,7] loops,[5] and grain boundaries[3] have been suggested to act as shallow traps.

In semiconductors, impurities form shallow levels for electrons and holes in the energy gap. In complete analogy, the long-range Coulomb field around negative impurities can be expected to bind positrons to Rydberg-like states with the binding energies determined by the positron effective mass. The shallow positron traps can also explain some of the difficulties, which have been met in applying the positron-annihilation technique to semiconductors.[8-14] In particular, compounds like GaAs contain impurities and various native defects at a level of $10^{15}-10^{16}$ cm^{-3}, and some of them may capture positrons into shallow levels.

Studies of vacancy defects in GaAs by positron-annihilation techniques have been a subject of increasing interest.[8-14] Although the experimental data obtained by different groups are similar, the interpretation varies considerably. A lot of problems are associated with the decomposition of the lifetime spectra into various annihilation states, which has proven to be difficult in as-grown or irradiated GaAs, especially at low temperatures.[11,14] Even when the decomposition is possible, the lifetime parameters do not follow the simple trapping model at temperatures below 200 K.[11]

The purpose of this work is to study systematically the temperature behavior of the positron-annihilation characteristics in GaAs in the range 10–600 K. We report, in addition to conventional lifetime measurements, the first positron-diffusion experiments in GaAs using a low-energy positron beam. This gives us a unique means of distinguishing between free and bound positron states in the cases where the annihilation characteristics of the two states are very similar.

Our lifetime results give evidence that below 200 K positrons are trapped, in addition to native vacancies, at shallow traps with no open volume. The existence of these shallow traps is confirmed by positron-diffusion-length measurements. The binding energy to the shallow traps is estimated to be 43±5 meV. For the origin of the shallow traps we suggest positron localization in the Rydberg states around negative acceptorlike centers, which are residual impurities or native defects in *n*-type GaAs.

The paper is organized as follows. In the next section the experimental details are given. Positron-lifetime and low-energy-beam results are presented in Secs. III and IV, respectively. In Sec. V the positron binding energy at shallow traps is determined and the nature of the shallow traps is discussed. Section VI concludes the paper.

II. EXPERIMENTAL

The samples used in our experiments were liquid-encapsulated Czochralski-grown GaAs crystals. They

 ©1989 The American Physical Society

TABLE I. The samples studied in this work and their carrier concentrations at room temperature.

Dopant atom	Conduction type	Carrier concentration (cm^{-3})
undoped	n	2.5×10^{14}
undoped	n	1.9×10^{15}
undoped	n	4.6×10^{15}
undoped	n	2.2×10^{16}
Sn	n	2.0×10^{17}
Te	n	3.2×10^{17}
Si	n	1.0×10^{18}

were all n type and are listed in Table I. The carrier concentrations at room temperature were determined using Hall measurements. In the undoped crystals the carriers are most probably from residual silicon impurities. Before the experiments the samples were etched at H_2SO_4:H_2O_2:H_2O (3:1:1) solution so that a layer of about 10 μm was removed from the sample surface.

For positron-lifetime measurements, two identical sample pieces of 10×10 mm^2 cut from the same wafer were sandwiched with a 40-μCi positron source. The source material was carrier-free ^{22}NaCl solution deposited onto a thin (1.1 mg/cm^2) nickel foil. Positron-lifetime measurements were carried out by a fast-fast lifetime spectrometer[15] with a time resolution of 225 ps (full width at half maximum). Each spectrum was measured for 3 h during which 1.5×10^6 pulses were accumulated. The increase of the counts up to 10^7 per one spectrum did not change our results significantly. After the subtraction of the source annihilations, the lifetime spectra were analyzed with one or two exponential decay components. The intensities of the annihilations in the source materials (182 ps, 9.1%; 450 ps, 7.0%) were found to be independent of temperature. A closed-cycle He cryocooler (Displex DE202) was used to vary the sample temperature between 10 and 300 K. The temperature stability was better than 0.5 K.

The positron-diffusion experiments were performed with a variable-energy (0–25 keV) positron beam under ultrahigh-vacuum conditions.[16] The positrons from a 70-mCi ^{58}Co source were thermalized in a backscattering W(110) moderator, by which a beam intensity of 8×10^5 s^{-1} was achieved. The positron-diffusion length was determined from the fraction of positrons, which after implantation into the sample diffused back to the surface. In the experiments the Doppler-broadened annihilation line-shape parameter S was measured as a function of the incident positron implantation energy. At each energy, 10^6 counts were collected to the photopeak of the spectrum with a Ge detector. The S parameter was defined as the area of the 2-keV-wide central region of the 511-keV line divided by the total area of the peak. The sample temperature could be varied from 120 to 700 K using liquid-nitrogen cooling and electron-beam heating.

III. POSITRON-LIFETIME RESULTS

A. Data analysis and one-defect trapping model

After the source corrections, the lifetime spectra are fitted to the sum of two exponential components:

$$n(t)=I_1e^{-\lambda_1 t}+I_2e^{-\lambda_2 t} \tag{1}$$

convoluted with the Gaussian resolution function of the spectrometer. The annihilation rate λ_i is the inverse of the positron lifetime, $\lambda_i=\tau_i^{-1}$. The decomposition is unambiguous if the lifetime values differ sufficiently, i.e., $\tau_2/\tau_1>1.5$. From the lifetimes and intensities I_i we also calculate the average lifetime

$$\tau_{av}=I_1\tau_1+I_2\tau_2 , \tag{2}$$

which is insensitive to the uncertainties in the decomposition and should coincide with the center of mass of the spectrum.

In a perfect crystal, free positrons annihilate with a single lifetime τ_b, which we have found to be 230 ps for GaAs.[10,11,13] In the presence of defects, positrons may get trapped and annihilate with a second lifetime τ_d, which for open-volume defects is always longer than the bulk lifetime. The positron trapping rate is proportional to the defect concentration c_d and is given by

$$\kappa=\mu_d c_d , \tag{3}$$

where μ_d is the so-called specific trapping rate.

In the simple trapping model, where only *one type of defect* is present and a trapped positron does not escape from the defect, the lifetime spectrum is two-exponential. The lifetimes and intensities are given by[17]

$$\tau_1^{-1}=\tau_b^{-1}+\kappa, \tag{4}$$

$$\tau_2=\tau_d , \tag{5}$$

$$I_2=1-I_1=\frac{\kappa}{\kappa+\lambda_b-\lambda_d}. \tag{6}$$

By applying Eqs. (4)–(6) to Eq. (2), the average lifetime τ_{av} can be expressed as

$$\tau_{av}=\frac{\lambda_b}{\lambda_b+\kappa}\tau_b+\frac{\kappa}{\lambda_b+\kappa}\tau_d. \tag{7}$$

The positron trapping rate κ can now be calculated from the decomposition of the lifetime spectra [Eq. (6)] or from the average lifetime [Eq. (7)]:

$$\kappa=\frac{I_2}{I_1}(\lambda_b-\lambda_d)=\frac{\tau_{av}-\tau_b}{\tau_d-\tau_{av}}\lambda_b . \tag{8}$$

If there is more than one type of positron trap present in the lattice, the analysis with more than two decay components is often not possible due to the high number of free parameters. However, in a two-component fit the longest lifetime τ_2 is usually clearly separated, while the shorter lifetime τ_1 becomes a superposition of the other decay components. In this case, Eqs. (4)–(8) of the simple trapping model can be used to check whether or not

the analysis is compatible with one defect type only. If only one type of trap is present and no detrapping occurs, the test lifetime $\tau_{1,\text{test}}$ calculated from Eqs. (4) and (8) using the experimental values of τ_{av} and τ_2,

$$\tau_{1,\text{test}}^{-1}=\tau_b^{-1}+\kappa=\tau_b^{-1}\left[1+\frac{\tau_{av}-\tau_b}{\tau_2-\tau_{av}}\right], \tag{9}$$

should coincide with the measured values of τ_1. If the experimental values are higher, then τ_1 is due to annihilations of both free positrons and those trapped at additional defects in the lattice.

B. Lifetime τ_2 and vacancy defects

All measurements performed in undoped n-type GaAs ($n=10^{14}-10^{16}$ cm^{-3}) show similar temperature behavior. The decomposition of the lifetime spectra in the GaAs ($n=2.2\times10^{16}$ cm^{-3}) is given as an example in Fig. 1. At all temperatures two lifetime components are given, although the decomposition becomes more difficult below 100 K.

The strong temperature dependence of the positron-lifetime parameters in Fig. 1 are typical of lightly n-type GaAs ($n=10^{15}-10^{16}$ cm^{-3}) studied in this work or earlier.[10,11] The lifetime τ_2, which is 292±3 ps at room temperature, is well above the bulk value of 230 ps and corresponds to a vacancy defect. Below 200 K it changes reversibly to 257±3 ps. Also, a strong increase in the lifetime τ_1 is seen: at low temperatures τ_1 approaches the bulk value of 230 ps. Below 100 K the two components are so close to each other that a free decomposition of the spectra becomes statistically more uncertain. In fact, the points from 10 to 60 K in Fig. 1 are based on a fit with fixed $\tau_2=257$ ps. The intensity I_2 decreases at low temperatures, also causing the *average* positron lifetime τ_{av} to decrease (see Fig. 5).

When the carrier concentration in n-type GaAs becomes higher than 10^{17} cm^{-3}, the reversible change in the second lifetime τ_2 is not observed, but a constant value of $\tau_2=257$ ps is found in the complete temperature range 10–300 K. As an example, the result of the GaAs ([Sn]$=2\times10^{17}$ cm^{-3}) sample are given in Fig. 2. The other two samples, GaAs ([Te]$=3.2\times10^{17}$ cm^{-3}) and GaAs ([Si]$=1\times10^{18}$ cm^{-3}), show qualitatively similar results independent of the dopant atom. At temperatures below 200 K the lifetime τ_1 increases, and the decrease in I_2 is again reflected to the average lifetime. Thus, apart from the differences in τ_2, a similar tendency is detected

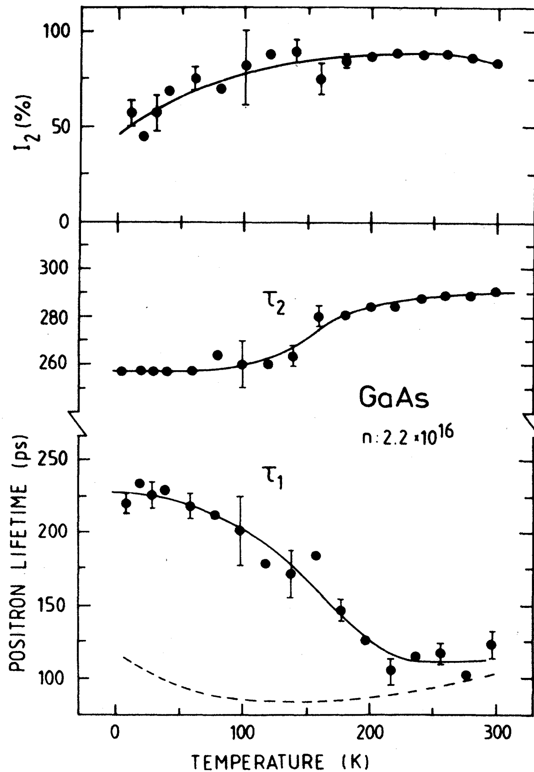

FIG. 1. Decomposition of the positron-lifetime spectra as a function of temperature in GaAs ($n=2.2\times10^{16}$ cm^{-3}). Below 60 K the results are based on a fit with τ_2 fixed to 257 ps. The dashed line indicates the values for τ_1 calculated from the one-defect trapping model [Eq. (9)]. It corresponds to the situation where only vacancy defects are present.

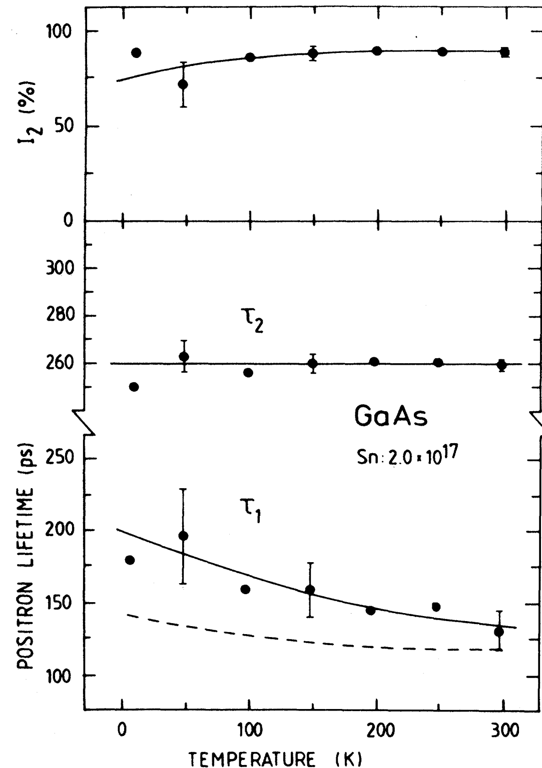

FIG. 2. Decomposition of the positron-lifetime spectra as a function of temperature in GaAS ([Sn]$=2.0\times10^{17}$ cm^{-3}). The dashed line indicates the values for τ_1 calculated from the one-defect trapping model [Eq. (9)]. It corresponds to the situation where only vacancy defects are present.

in the decomposition of both doped and undoped n-type GaAs, and due to the strong increase of the lifetime τ_1 the two-component analysis becomes difficult in all samples at temperatures below 100 K.

The details of the temperature dependence in the lifetime τ_2 associated with the positrons trapped at vacancies are not discussed here, but the complete analysis will be published separately.[18] The interpretation of Corbel *et al.*[11] is based on the direct relation between the Fermi level and the lifetime τ_2 in n-type GaAs. At low temperatures the Fermi level is close to the conduction band and the lifetime $\tau_2=257$ ps is observed. With increasing temperature the Fermi level moves down towards the midgap region and the $\tau_2=257$ ps lifetime is replaced by the $\tau_2=292$ ps lifetime. This transition is attributed to the $V_{\mathrm{As}}^{2-}\rightarrow V_{\mathrm{As}}^{1-}$ ionization of the As vacancy. At the intermediate temperature an equilibrium between the annihilation states 257 and 292 ps is found. At high n-type doping level the vacancy lifetime of 257 ps is found at any temperature.

The increase of the lifetime τ_1 at low temperatures (see Figs. 1 and 2) is independent of the 257→292 ps transition of the lifetime τ_2. The physical process behind the behavior of τ_1 is the scope of the present paper.

C. Lifetime τ_1 and shallow traps

To test the validity of the simple one-defect trapping model we have compared the experimental τ_1 values to those calculated from the model using Eq. (9) with the bulk lifetime $\tau_b=230$ ps. The calculated values $\tau_{1,\mathrm{test}}$ as a function of temperature are presented as dashed lines in Figs. 1 and 2.

The difference between the experimental τ_1 and the values $\tau_{1,\mathrm{test}}$ calculated from the one-defect trapping model [Eq. (9)] is evident in Figs. 1 and 2. Below 200 K the experimental τ_1 values in all samples are systematically 50–100 ps larger than expected from Eq. (9). This indicates that the one-defect trapping model is valid only at temperatures close to 300 K. In addition to the vacancy defects (257 or 292 ps), other positron traps are active at low temperatures. They modify the behavior of the lifetime τ_1 in such a way that the one-defect trapping model fails to explain the decompositions of the lifetime spectra.

The shorter-lifetime component τ_1 is studied in more detail in Fig. 3, which shows the results in three undoped n-type GaAs samples from a *completely free* two-component analysis of the spectra. The large error bars indicate that the two lifetimes in the spectra are very close to each other, and a high-resolution spectrometer is needed for decomposition. In addition to the strong increase below 200 K, the results show a saturation level of τ_1, which is equal to the lifetime for free positrons in bulk $\tau_b=230$ ps. In all three samples the second component τ_2 of 257–292 ps from vacancy defects is still observable and the average lifetime is clearly higher than the bulk value. The spectra thus consist of at least two lifetime components despite the uncertainties in the decomposition procedure.

The increase of τ_1 is independent of the 257→292 ps

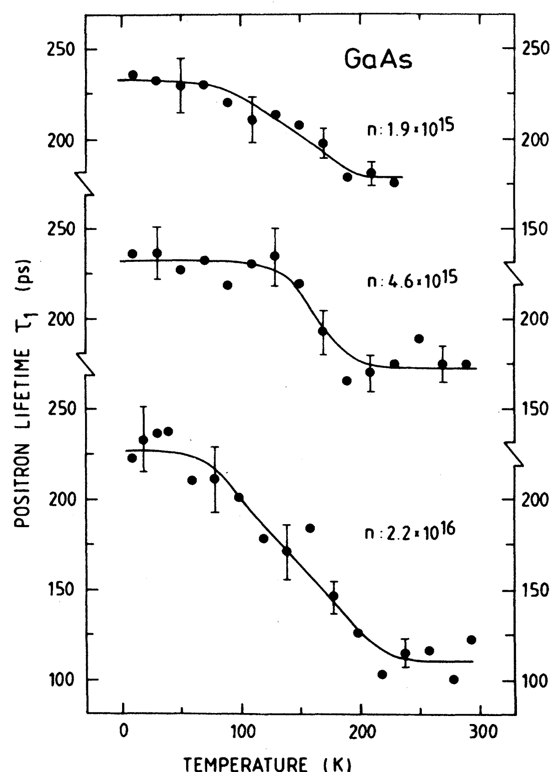

FIG. 3. Temperature dependence of the lifetime component τ_1 in three undoped n-type GaAs samples. The results are based on unrestricted fits.

transition in τ_2. In the three undoped GaAs samples in Fig. 3, τ_1 increases to 230 ps between 200 and 100 K, while the transition 257→292 ps occurs at 50–100 K in GaAs ($n=1.9\times10^{15}$ cm^{-3}), at 60–120 K in GaAs ($n=4.6\times10^{15}$ cm^{-3}), and at 90–170 K in GaAs ($n=2.2\times10^{16}$ cm^{-3}).[18] In the doped samples τ_2 stays constant, but τ_1 still increases with decreasing temperature.

The behavior of τ_1 in Figs. 1–3 can be understood in the following way. The first lifetime component is a superposition of annihilations in the free state [$\tau_1'=\tau_b/(1+\kappa\tau_b)$ from Eq. (4)] and in the additional traps ($\tau_1''=\tau_{\mathrm{st}}$), which are effective only at low temperatures. Then, at the saturation of $\tau_1=\tau_{\mathrm{st}}$, the annihilations in the free state are completely suppressed, and all positrons are trapped either in the vacancies ($\tau_2=257$–292 ps) or in the additional traps. This saturation level of $\tau_1=\tau_{\mathrm{st}}=230$ ps coincides with the bulk lifetime, indicating that the additional traps have no open volume. The behavior of τ_1 as a function of temperature can then be ascribed to thermally assisted positron detrapping from these shallow traps, which have a binding energy comparable to the thermal energies at 200–300 K.

The behavior of the lifetime spectra and particularly its shorter component τ_1 found in this work are identical to the earlier results on GaAs by Kerr *et al.*,[19] Dannefaer

et al.,[9] and Corbel *et al.*[11] Although not emphasized before, the inadequacy of the simple trapping model below 200 K can also be seen from these previous results. The direct identification of the shallow traps by positron-lifetime spectroscopy is, nevertheless, very difficult because the actual annihilation parameters measured are very similar in the bulk and in the shallow traps. Therefore, only indirect information can be deduced by the validity test of the one-defect trapping model. The direct observation of the positron trapping and thermal detrapping becomes possible by positron-diffusion measurements, where the experimental signal is not the open volume of the lattice, but the positron-diffusion length and the total trapping rate.

IV. POSITRON-DIFFUSION RESULTS

A. Data analysis

Positrons can be implanted at various depths into the sample by varying the incident energy of the positron beam. After rapid thermalization, positrons start to diffuse. They may annihilate in the sample interior or diffuse back to the entrance surface and annihilate there. The fraction of the annihilations on the surface is determined by the implantation depth and the diffusion length.

The experimental Doppler parameter $S(E)$ measured as a function of positron incident energy E is a superposition of the different S-parameter values for the annihilations on the sample surface (S_{surf}) and in the interior (S_{int}):

$$S(E)=j(E)S_{surf}+[1-j(E)]S_{int}, \tag{10}$$

where $j(E)$ is the fraction of positrons diffusing to the entrance surface. In the case of homogeneous vacancy-defect distribution there is a competition in the sample interior between annihilations in the bulk (S_{bulk}) and in the vacancies (S_{vac}), and we get

$$S_{int}=\frac{\kappa}{\lambda_b+\kappa}S_{vac}+\frac{\lambda_b}{\lambda_b+\kappa}S_{bulk}, \tag{11}$$

where $\lambda_b=1/\tau_b$ is the free-positron annihilation rate and κ is the trapping rate into the vacancies. Thus S_{int} is a sample-dependent parameter, which can be measured at high incident energies. The backdiffusion probability $j(E)$ is obtained from the positron-diffusion–annihilation equation[20]

$$D_+\nabla^2 n(z)-(\lambda_b+\kappa)n(z)+p(z)=0 , \tag{12}$$

which yields

$$j(E)=D_+\nabla n(0)=\int_0^\infty p(z,E)e^{-z/L_+}dz. \tag{13}$$

Here $n(z)$ is the quasistationary positron distribution, D_+ the diffusion constant, and L_+ the diffusion length:

$$L_+=(D_+\tau_{eff})^{1/2} \tag{14}$$

with

$$\tau_{eff}^{-1}=\lambda_b+\kappa . \tag{15}$$

For the positron-implantation profile in GaAs we use[21]

$$p(z,E)=2(z/z_0^2)e^{-(z/z_0)^2} , \tag{16}$$

where

$$z_0=(70\ \text{Å})[E/(1\ \text{keV})]^{1.6} . \tag{17}$$

Often the diffusion length is also given by an E_0 parameter:[20]

$$L_+=(70\ \text{Å})[E_0/(1\ \text{keV})]^{1.6} , \tag{18}$$

where E_0 is approximately the half-width of the $S(E)$ curve.

In the analysis of the positron-diffusion measurements, the experimental $S(E)$ points were fitted to Eq. (10) with three free parameters S_{surf}, S_{int}, and E_0. As can be seen by comparing Eqs. (7) and (11), the asymptotic value of the S parameter (S_{int}) at high incident energies is directly proportional to the positron average lifetime τ_{av}. Thus defect-specific information can also be extracted from the slow-positron data.

B. Diffusion results

Figure 4 shows the fitted values of S_{int} and positron-diffusion length L_+ as well as the positron lifetime in GaAs ($n=2.5\times10^{14}$ cm^{-3}). The lifetime measurements show no positron trapping at any temperature. The constant value of the positron lifetime is very close to the bulk lifetime 230 ps, which indicates that no trapping at vacancy-type defects occurs at any temperature. The same tendency is observed in the S_{int} parameter. It shows only a small linear increase due to lattice dilatation, which is typical for annihilations in the bulk.

The temperature behaviors of the parameters L_+, τ_{av}, and S_{int} in the GaAs ($n=2.2\times10^{16}$ cm^{-3}) are shown in Fig. 5. The detailed decomposition of the corresponding lifetime spectra has already been shown in Fig. 1. The S_{int} parameter again follows completely the behavior of the average lifetime. The maximum of S_{int} is observed at the same temperature as the maximum in τ_{av}. Both parameters decrease above room temperature, which is due to the gradual suppression of the positron trapping above 300 K, ascribed to the ionization $V_{As}^{1-}\rightarrow V_{As}^{0}$ of the As vacancy.[11]

We see from above that the same physical phenomena contribute to the measured positron parameters in both slow-positron and lifetime experiments. Thus we expect that the positron-diffusion data obtained from the beam measurements can be very reliably interpreted. The experimental positron-diffusion parameters E_0 as a function of temperature and the corresponding diffusion lengths L_+ from Eq. (18) are presented in Figs. 4 and 5.

At temperatures higher than 300 K the positron-diffusion length L_+ is seen to be about 1500 Å and almost constant in both samples. Below room temperature a radical change in L_+ is observed, as the diffusion length drops to 700 Å. The dashed line in Figs. 4 and 5 indicates the temperature dependence of the positron-diffusion length $L_+=(D_+\tau_{eff})^{1/2}\propto T^{-1/4}$, corresponding to the standard theory of positron diffusion, where the

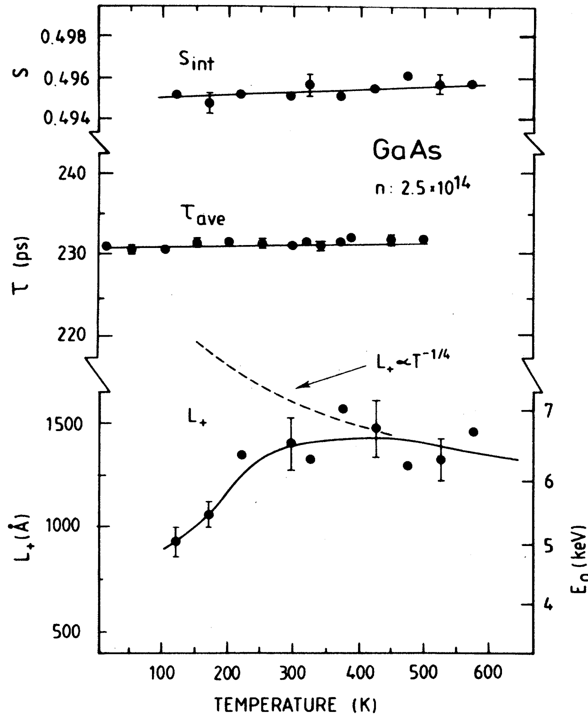

FIG. 4. Results of the positron-beam experiments in GaAs ($n=2.5\times10^{14}$ cm^{-3}). In addition to diffusion length L_+ and Doppler parameter S_{int} in the sample interior, the average positron lifetime τ_{av} as a function of temperature is given. The dashed line indicates the diffusion length of free positrons based on the positron scattering from acoustic phonons.

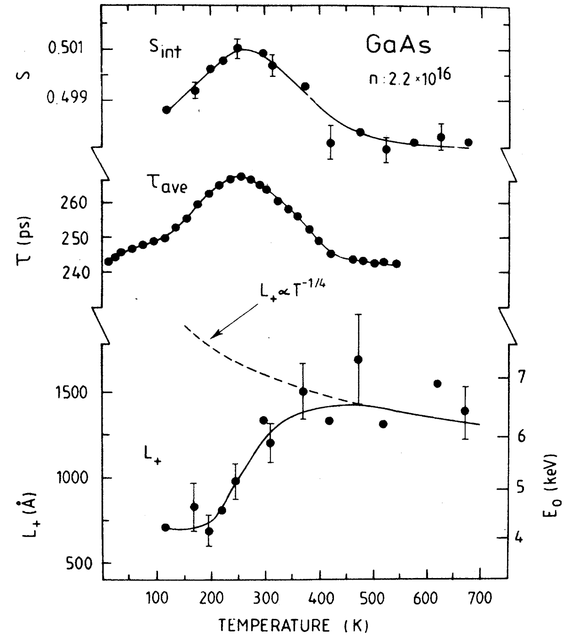

FIG. 5. Results of the positron-beam experiments in GaAs ($n=2.2\times10^{16}$ cm^{-3}). In addition to diffusion length L_+ and Doppler parameter S_{int} in the sample interior, the average positron lifetime τ_{av} as a function of temperature is given. The dashed line indicates the diffusion length of free positrons based on the positron scattering from acoustic phonons.

diffusion is limited by the positron scattering from acoustic phonons with $D_+ \propto T^{-1/2}$.[22,23] The measured diffusion lengths in GaAs thus show clear deviations from the $D_+ \propto T^{-1/2}$ model at temperatures below 400 K.

The decrease of the positron-diffusion length L_+ at low temperatures means the decrease of $\tau_{eff}=(\lambda_b+\kappa)^{-1}$, i.e., a strong increase in the trapping rate κ. However, the positron traps in the GaAs ($n=2.5\times10^{14}$ cm^{-3}) sample are not vacancy defects, as both τ_{av} and S_{int} in Fig. 4 have values typical of annihilations in the bulk.

In the GaAs ($n=2.2\times10^{16}$ cm^{-3}) sample in Fig. 5, the decrease of L_+ between 400 and 250 K coincides with the increasing positron trapping into vacancies, as seen in the increase of τ_{av} and S_{int}. Below 250 K the diffusion length L_+ continues to decrease, although τ_{av} and S_{int} start to decrease. The trapping rates calculated from both positron-lifetime [Eq. (8)] and diffusion-length [Eq. (15)] results coincide well at temperatures above 250 K. Below 250 K the trapping rates from Eq. (15) become clearly higher than those from Eq. (8) based on the one-defect trapping model. This leads us to conclude that in this sample the strong decrease of the positron-diffusion length must also reflect positron trapping, which is not visible in average lifetime or Doppler parameter and which depends strongly on the measurement temperature.

When the positron-diffusion experiments are compared with the positron-lifetime results, it is directly observed that the decrease in the diffusion length and the failure of the one-defect trapping model occurs at the same temperature range, which is between 200 and 300 K in any sample. The decomposition of the lifetime spectra at low temperatures is disturbed by an additional lifetime component, which has a value very close to the free annihilation in the bulk. The interpretation to connect this with positron trapping to shallow traps is clearly confirmed by the positron-diffusion-length measurements: at the same temperature where the one-defect trapping model fails to explain the decomposed lifetime spectra, the positron-diffusion length is noticed to decrease to half of the value corresponding to free diffusion. This trapping is also observed in GaAs ($n=2.5\times10^{14}$ cm^{-3}), where both Doppler and lifetime measurements show annihilations in the bulk, indicating that the traps are not of vacancy type. Thus the lifetime, Doppler, and positron-diffusion measurements are all consistent with the physical picture that a large number of shallow positron traps is present in GaAs.

V. DISCUSSION

A. Determination of the binding energy

The results with three different experimental positron methods presented in this work provide a simple way of

understanding the behavior of the lifetime spectra at low temperatures: in addition to the vacancy-type defects, some other traps with both positron lifetime and Doppler broadening very close to the bulk values affect the positron motion at low temperatures. These shallow traps are directly visible with positron-diffusion-length measurements, and they are responsible for the observed difficulties in the analysis of the lifetime experiments. A high-resolution positron-lifetime spectrometer is needed to reliably distinguish between the two dominant lifetimes at low temperatures, 230 ps for shallow traps and 257 ps for vacancies. The changes in the structure of the lifetime spectra between 100 and 200 K and the increase in the positron-diffusion length at the same temperature range can thus be understood with thermal positron detrapping from the shallow traps.

1. Positron-lifetime results

To analyze the positron-lifetime data quantitatively we have adopted the method proposed by Manninen and Nieminen.[24] A thermodynamic approach to the positron detrapping from a defect gives for the ratio of the detrapping (δ) and trapping (κ_{st}) rates

$$\frac{\delta}{\kappa_{st}}=\frac{1}{c_{st}}\left[\frac{m^*}{2\pi\hbar^2}\right]^{3/2}(k_BT)^{3/2}\exp\left[-\frac{E_b}{k_BT}\right] \tag{19}$$

where E_b is a binding energy of the positron to the shallow traps with the concentration c_{st} and m^* is the positron effective mass. This formula can be fitted to the experimental data, if the corresponding trapping equations are solved to determine the transition rates δ and κ_{st}. We have applied a three-state trapping model, which consists of annihilations as free positrons, trapping to vacancies with trapping rate κ_v, and trapping and detrapping to shallow traps with rates κ_{st} and δ, respectively. Assuming that in the two-component analysis of the lifetime spectra the longest component corresponding to annihilations in vacancies is clearly separated from the others, the solution of the kinetic trapping equations gives an experimental formula for the positron detrapping rate:[5]

$$\frac{\delta}{\kappa_{st}}=\left[\frac{I_2}{I_1\kappa_v-I_2(\lambda_b-\lambda_2)}-\frac{1}{\kappa_{st}}\right](\lambda_{st}-\lambda_2), \tag{20}$$

where $\tau_2=\lambda_2^{-1}$ and I_2 are the lifetime and the intensity of the longest component in the lifetime spectra and $\lambda_{st}=\tau_{st}^{-1}$ and $\lambda_b=\tau_b^{-1}$ are the annihilation rates in the shallow traps and in the bulk crystal, respectively. In addition, we assume $\lambda_{st}=\lambda_b$.

In order to get the experimental detrapping rates using Eq. (20), knowledge of the temperature dependencies of the trapping rates κ_v and κ_{st} is needed. Unfortunately, this causes some difficulties, because the simultaneous determination of the three parameters κ_v, κ_{st}, and δ from the experimental data is impossible. In analogy to free-carrier capture at defects,[25] various positron-trapping mechanisms leading to different temperature dependencies are possible and determined by the charge state of the defect and the Fermi-level position of the sample.[26] To simplify, we assume that the trapping rates κ_{st} and κ_v do not depend on temperature and estimate the value of κ_{st} at 0 K (no thermal detrapping) and κ_v at 300 K (no trapping to shallow traps). Then the behavior of the detrapping rate in Eq. (20) is completely controlled by the intensity of the vacancy component I_2.

Figure 6 shows the Arrhenius plots of the measured detrapping rates from Eq. (20) in GaAs ([Sn]$=2.0\times10^{17}$ cm^{-3}), GaAs ([Te]$=3.2\times10^{17}$ cm^{-3}), and GaAs ([Si]$=1.0\times10^{18}$ cm^{-3}) samples. The solid lines are the fits of Eq. (19) to the experimental data with $E_b=43$ meV. In addition to the shallow-trap behavior described earlier, vacancies with positron lifetime 260 ps were found at any temperature because of the high *n*-type doping. In the final analysis the 260-ps component was fixed to decrease the statistical uncertainties in the fitting. The intensity of the vacancy component I_2 was constant between 150 and 300 K, but below 150 K a decrease in I_2 was observed. Our experimental lifetime results are consistent with the earlier measurements by Dannefaer

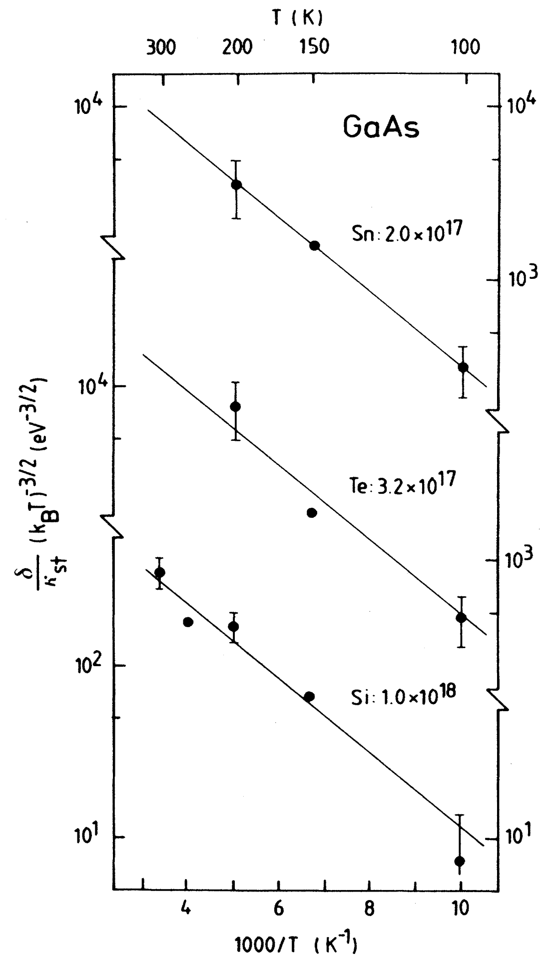

FIG. 6. The ratio of the detrapping and trapping rates in heavily doped *n*-type GaAs calculated from the decompositions of the lifetime spectra using Eq. (20). The solid lines are the fits of Eq. (19) to the experimental data with $E_b=43$ meV.

et al.[9] and Corbel *et al.*[11]

The slopes in Fig. 6 are about the same for all samples. The analysis yields binding energies in the range $E_b = 0.040-0.045$ eV. The detrapping rate δ is found to coincide with the trapping rate κ_{st} at 150 K, where the lifetime spectrum changes most. The determination of the trapping rate κ_{st} is found to be very insensitive to the fraction δ/κ_{st}, at least when κ_{st} is large ($\kappa_{st} > 5$ ns^{-1}) [see Eq. (20)]. The error in E_b due to the systematically wrong choice of κ_{st} was estimated to be less than 20%. For example, if we vary the value of κ_{st} from 6 to 90 ns^{-1} when analyzing the results of GaAs ([Si]$=1\times10^{18}$ cm^{-3}) sample, the corresponding variation in E_b is less than ±5 meV. Thus we believe that, although we have omitted the temperature dependencies of κ_{st} and κ_v, we get a reasonable estimate to E_b.

2. *Positron-diffusion results*

To perform a quantitative analysis of the positron-diffusion results the detrapping rate has to be added to the diffusion-annihilation equation (12). Instead of Eq. (15), the quasistationary solution then yields for the effective lifetime τ_{eff} (Ref. 20)

$$\tau_{eff}^{-1} = \lambda_b + \kappa_v + \frac{\kappa_{st}\lambda_{st}}{\delta + \lambda_{st}} . \tag{21}$$

Using Eqs. (14) and (18) the ratio δ_{st}/κ_{st} can then be expressed in terms of the measured parameter E_0:

$$\frac{\delta}{\kappa_{st}} = \frac{E_0^{3.2}}{E_{0,b}^{3.2} - \left[1 + \frac{\kappa_v}{\lambda_b}\right] E_0^{3.2}} - \frac{\lambda_b}{\kappa_{st,}} , \tag{22}$$

where $E_{0,b}$ is the value for the *free*-positron diffusion, assumed to be proportional to $L_+^{1/1.6} \propto (T^{-1/4})^{1/1.6}$ [see Eq. (18)]. In Eq. (22), $\lambda_{st} = \lambda_b$ is again assumed. The estimation of κ_{st} from the saturation of E_0 ($\delta/\kappa_{st} \to 0$, when $T \to 0$) yields values of the range $\lambda_b/\kappa_{st} \sim 0.1$, which indicates that the last term in Eq. (22) does not have a large effect on δ/κ_{st}.

The results of the detrapping analysis of the GaAs ($n = 2.5\times10^{14}$ cm^{-3}) and GaAs ($n = 2.2\times10^{16}$ cm^{-3}) samples measured with the slow-positron beam are presented in Fig. 7. In GaAs ($n = 2.5\times10^{14}$ cm^{-3}) no positron trapping into vacancies was found, and Eq. (22) is thus considerably simplified by substituting $\kappa_v = 0$. The trapping rate κ_v for the GaAs ($n = 2.2\times10^{16}$ cm^{-3}) sample is assumed to be temperature independent and it is calculated from the E_0 value at 300 K.

The Arrhenius plot for the GaAs ($n = 2.5\times10^{14}$ cm^{-3}) sample shows that the experimental detrapping rate follows the functional shape of Eq. (19) well. The slopes in Figs. 6 and 7 are very close to each other, and from the slow-positron data for the GaAs ($n = 2.5\times10^{14}$ cm^{-3}) sample a value of $E_b = 43\pm6$ meV is obtained for the positron binding energy in the shallow traps. The analysis for the GaAs ($n = 2.2\times10^{16}$ cm^{-3}) sample results in a larger scatter of the δ/κ_{st} values. The reason for this is the vacancy trapping κ_v in Eq. (22) and the uncertainties

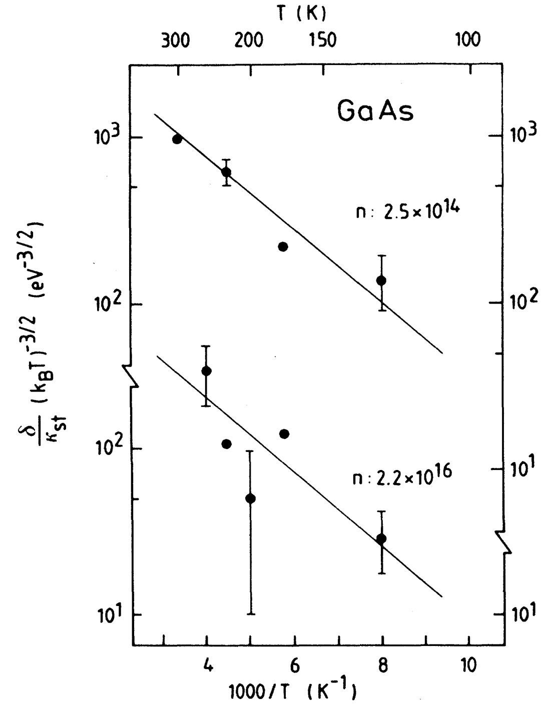

FIG. 7. The ratio of the detrapping and trapping rates in undoped n-type GaAs calculated from the positron-beam data using Eq. (22). The solid lines are the fits of Eq. (19) to the experimental data with $E_b = 43$ meV.

in its value, especially because the vacancy lifetime transition 257→292 ps coincides with the onset of the detrapping from the shallow traps. Nevertheless, the Arrhenius plot for the GaAs ($n = 2.2\times10^{16}$ cm^{-3}) sample indicates the same slope as in the other samples with a rough estimate of $E_b \sim 40$ meV for the binding energy.

In conclusion, our detrapping analysis shows that both positron-lifetime and diffusion-length measurements give consistent results yielding to the positron binding energy $E_b = 43\pm5$ meV in the shallow traps. This value is close to the thermal energy of the positron at 250 K ($\frac{3}{2}k_BT = 32$ meV), where the detrapping probability raises to a value higher than the trapping rate κ_{st}. We thus believe that the same quantitative results obtained independently by two different positron methods give strong experimental evidence of positron localization in shallow traps in n-type GaAs at temperatures below 250 K.

B. The nature of the shallow traps

The detailed atomic configuration of the shallow traps cannot be deduced from the positron measurements. Because the positron lifetime at the shallow traps is equal to the bulk value, the traps do not contain open volume and they are not of vacancy type. An impurity atom or a point defect with a negative charge can induce the observed shallow positron state. Being a positive particle, a positron can get localized in a Rydberg-like state of the

Coulomb field around a negatively charged center, and the situation is analogous to the binding of a hole to an acceptor atom. The binding energy to a Rydberg state can be estimated with a simple formula:[27]

$$E_b = \frac{13.6 \text{ eV}}{\epsilon^2} \left[\frac{m^*}{m_e} \right] \frac{1}{n^2} , \tag{23}$$

where ϵ is the dielectric constant of the material, m^* is the effective mass of the positron, and n is the quantum number. The positron effective band mass in all solids is very close to its free mass.[28] If we take $m^*=m_e$ and $\epsilon=12.9$ in GaAs, Eq. (23) gives $E_b=80$ meV for the binding energy in the first Rydberg state ($n=1$). This is of the same order of magnitude as we obtained from our positron-detrapping analysis. In fact, the agreement can be even better, because the detrapping may also occur from excited states, and the experimental value of $E_b=43$ meV represents an *average* binding energy over several Rydberg states.

The binding energies of holes to acceptor atoms range typically between 20 and 30 meV in GaAs, whereas the corresponding values for electrons to donor atoms are 3–6 meV.[29] The effective mass for holes and electrons are $m_h^*=0.5m_e$ and $m_e^*=0.1m_e$,[29] respectively. To a first approximation, the binding energy of a carrier is directly proportional to its density-of-states effective mass through Eq. (23). Thus our experimental binding energy for positron $E_b=43$ meV is in good agreement with values obtained for electrons and holes, when it is scaled with the effective-mass ratios.

The bulk GaAs crystals are known to contain both various residual impurities and native defects at the level of $10^{15}-10^{17}$ cm^{-3}.[30] In undoped material, $EL2$ is an important native defect, the atomic configuration of which is still under discussion. $EL2$ must be compensated by some ionized negative acceptors. These could be residual impurities like C_{As}^-, Zn_{Ga}^-, or Mg_{Ga}^-. Among the native defects, gallium antisite Ga_{As}^- is the one which is generally believed to exist as negatively charged, when the Fermi level is in the upper part of the energy gap.[31] As a typical example, our sample GaAs ($n=2.2\times10^{16}$ cm^{-3}) has been characterized also by electrical and optical measurements.[32] It contains $EL2^0$ centers 2×10^{16} cm^{-3}. The number of ionized acceptors is 6×10^{16} cm^{-3} at 300 K.

The doped GaAs always contains compensating centers, which in n-type material are negatively charged acceptors. For example, in Si doping a small fraction of silicon impurities may also occupy the As site forming Si_{As}^- centers. Thus there are many candidates, both impurities and native defects, for the negative centers acting as shallow traps for positrons.

The total concentration 10^{16} cm^{-3} of the ionized acceptorlike centers obtained from the Hall measurement can be used to estimate the specific trapping rate of the positrons to the Rydberg states. When the detrapping probability δ approaches zero ($T<100$ K), the trapping rate κ_{st} typically gets values of the order of 30 ns^{-1}. Using Eq. (3), the specific trapping rate μ_{st} at the 0-K limit becomes of the order of 10^{17} s^{-1}. This value is much higher than the specific trapping rates into point defects in metals.[1,2,17] It is comparable to the giant capture rates for electrons and holes at charged centers in semiconductors, where the dominant trapping mechanism is a phonon cascade emission.[25] Also for negatively charged vacancies in silicon, a specific trapping rate of the order of $10^{17}-10^{18}$ s^{-1} has recently been measured at low temperatures.[26]

To summarize, the positron localization around a negative point charge is possible and plausible at low temperatures, and it gives us a reasonable model for the interpretation of our experimental results.

VI. CONCLUSIONS

In this paper we have systematically studied positron annihilation in n-type GaAs at low temperatures. A large variety of samples with different dopant atoms in a concentration range $10^{14}-10^{18}$ cm^{-3} were investigated. In addition to lifetime experiments, positron-diffusion-length measurements in GaAs were also performed.

The lifetime measurements below 200 K show that a simple positron-trapping model with one type of vacancy defect is not sufficient to explain the decomposition of the lifetime spectra. An additional component with a lifetime very close to the bulk value is found at low temperatures, and a high-resolution spectrometer was needed to reliably separate it from the vacancy signals. A thermal detrapping from this annihilation state was observed between 100 and 200 K.

The low-energy positron-beam measurements reveal a strong decrease in the positron-diffusion length at temperatures below 300 K, although annihilation characteristics have values typical for the bulk. Consistently with the lifetime results, the phenomena can be explained with positron localization at shallow traps.

The analysis of both the lifetime and beam data in terms of the positron detrapping from shallow traps gives a binding energy of $E_b=43\pm5$ meV for the localized positron. The positron localization is associated with the Rydberg states around negative acceptor-type centers, and the positron binding energy is comparable to the shallow levels of electrons and holes in GaAs. These negative centers are formed of residual impurities, native defects, and in n-type-doped GaAs also of compensating centers, which in bulk GaAs always exist at concentrations higher than 10^{15} cm^{-3}. The specific trapping-rate values at 0 K are of the order of 10^{17} s^{-1}, which are comparable to the carrier-capture rates at charged defects by a phonon cascade mechanism.

ACKNOWLEDGMENTS

The authors are grateful for the invaluable help of J. Mäkinen and P. Huttunen during the slow-positron measurements.

[1]*Positrons in Solids,* Vol. 12 of *Topics in Current Physics,* edited by P. Hautojärvi (Springer, Heidelberg, 1979).
[2]*Positron Solid State Physics,* edited by W. Brandt and A. Dupasquier (North-Holland, Amsterdam, 1983).
[3]I. K. MacKenzie, Phys. Rev. B **16**, 4705 (1977).
[4]P. J. Schultz, K. G. Lynn, I. K. MacKenzie, Y. C. Jean, and C. L. Snead, Phys. Rev. Lett. **44**, 1623 (1980).
[5]B. Pagh, H. E. Hansen, B. Nielsen, G. Trumphy, and K. Petersen, Appl. Phys. A **33**, 255 (1984).
[6]S. Linderoth and C. Hidalgo, Phys. Rev. B **36**, 4054 (1987).
[7]L. C. Smedskjaer, M. Manninen, and M. J. Fluss, J. Phys. F **10**, 2237 (1980).
[8]M. J. Puska, O. Jepsen, O. Gunnarsson, and R. M. Nieminen, Phys. Rev. B **34**, 2965 (1986).
[9]S. Dannefaer, B. Hogg, and D. Kerr, Phys. Rev. B **30**, 3355 (1984).
[10]G. Dlubek, O. Brümmer, F. Plazaola, and P. Hautojärvi, J. Phys. C **19**, 331 (1986).
[11]C. Corbel, M. Stucky, P. Hautojärvi, K. Saarinen, and P. Moser, Phys. Rev. B **38**, 8192 (1988).
[12]S. Dannefaer and D. Kerr, J. Appl. Phys. **60**, 591 (1986).
[13]G. Dlubek and R. Krause, Phys. Status Solidi **102**, 443 (1987).
[14]P. Hautojärvi, P. Moser, M. Stucky, C. Corbel, and F. Plazaola, Appl. Phys. Lett. **48**, 809 (1986).
[15]A. Vehanen and K. Rytsölä, in *Positron Solid State Physics,* edited by W. Brandt and A. Dupasquier (North-Holland, Amsterdam, 1983), pp. 659–678.
[16]J. Lahtinen, A. Vehanen, H. Huomo, J. Mäkinen, P. Huttunen, K. Rytsölä, M. D. Bentzon, and P. Hautojärvi, Nucl. Instrum. Methods B **17**, 73 (1986).
[17]R. N. West, in *Positrons in Solids,* Vol. 12 of *Topics in Current Physics,* edited by P. Hautojärvi (Springer, Heidelberg, 1979), pp. 89–144; A. Vehanen, P. Hautojärvi, J. Johansson, J. Yli-Kauppila and P. Moser, Phys. Rev. B **25**, 762 (1982).
[18]K. Saarinen, P. Hautojärvi, R. Krause, and G. Dlubek (unpublished).
[19]D. P. Kerr, S. Kupca, and B. G. Hogg, Phys. Lett. **88**, 429 (1982).
[20]K. G. Lynn, in *Positron Solid State Physics,* edited by W. Brandt and A. Dupasquier (North-Holland, Amserdam, 1983), pp. 609–643; P. J. Schultz and K. G. Lynn, Rev. Mod. Phys. **60**, 701 (1988).
[21]A. Vehanen, K. Saarinen, P. Hautojärvi, and H. Huomo, Phys. Rev. B **35**, 4606 (1987).
[22]B. Bergensen, E. Pajanne, P. Kupica, M. J. Stott, and C. H. Hodges, Solid State Commun. **15**, 1377 (1974).
[23]H. Huomo, A. Vehanen, M. D. Bentzon, and P. Hautojärvi, Phys. Rev. B **35**, 8252 (1987).
[24]M. Manninen and R. M. Nieminen, Appl. Phys. A **26**, 93 (1981).
[25]M. Jaros, *Deep Levels in Semiconductors* (Hilger, Bristol, 1982); B. K. Ridley, *Quantum Processes in Semiconductors* (Clarendon, Oxford, 1982).
[26]J. Mäkinen, C. Corbel, P. Hautojärvi, P. Moser, and F. Pierre, Phys. Rev. B (to be published).
[27]N. W. Ashcroft and N. D. Mermin, *Solid State Physics* (Holt-Saunders, New York, 1976), p. 579.
[28]O. V. Boev, M. J. Puska, and R. M. Nieminen, Phys. Rev. B **36**, 7786 (1987).
[29]S. M. Sze, *Physics of Semiconductor Devices* (Wiley, New York, 1981).
[30]*Deep Centers in Semiconductors: A State of the Art Approach,* edited by S. T. Pantelides (Gordon and Breach, New York, 1986).
[31]G. Baraff and M. Schlüter, Phys. Rev. Lett. **55**, 1327 (1985).
[32]G. Dlubek, A. Dlubek, R. Krause, O. Brümmer, K. Friedland, and R. Rentzsch, Phys. Status Solidi A **106**, 419 (1988).